



# Estimating tectonic thinning of a layer using core data and pure shear/simple shear faulting models

S. Pallesen<sup>a,\*</sup>, S. Ottesen<sup>b</sup>

<sup>a</sup>*Statoil, N-4035 Stavanger, Norway*

<sup>b</sup>*Statoil, Arkitekt Ebbels vei 10, Rotvoll, N-7005 Trondheim, Norway*

Received 26 June 2000; revised 5 July 2001; accepted 25 August 2001

## Abstract

Tectonic thinning of a layer is estimated here using two different models: (i) a pure shear model with conjugate microfaults, and (ii) a simple shear model in which the microfaults dip in the same direction. These end-member bulk models may be interpolated in terms of a stretching factor. Formulas for use of deviated well data in calculating tectonic thinning are defined. The input to the modelling is data from structural core logging.

The main data is the number of microfaults and the mean displacement associated with them. The formulas are derived as if the microfaults were regularly spaced and all with the same (mean) displacement and applied to data showing variability. For pure shear this makes no difference, and for simple shear this is an approximation containing the assumption that the local layer (reservoir) has somewhat constant mechanical properties.

This type of modelling is useful for hydrocarbon exploration and production for the case where a local layer (reservoir) thickness anomaly at the well position—caused by microfaulting—is suspected. By identifying this, a more correct well-to-seismics layer thickness calibration can be carried out. A case study from the North Sea is presented at the end of the paper. © 2002 Published by Elsevier Science Ltd.

*Keywords:* Geometry; Non-continuum strain analysis; Faults; Interpolation (equation of state); Two-dimensional analysis

## 1. Introduction

In estimating hydrocarbon volumetrics, the bed thickness in a well position is used to calibrate bed thickness from seismic data. The bed orthogonal thickness is used in volume calculations. However, the bed thickness in well position may not be representative because of local intense faulting. At the same time, seismic resolution of reservoir levels may be poor. Improved use of well data for better structural control of the seismic interpretation has been studied by e.g. Hesthammer (1998), and is also the aim of the present paper.

Below is presented a simple method of estimating a representative thickness of a layer (reservoir) for the case of local, intense faulting at and close to a well. It is assumed that a two-dimensional (2D) analysis is applicable, and that ductile layer thinning is negligible—formation of microfaults or deformation bands may take place at high

porosities (Underhill and Woodcock, 1987; Antonellini et al., 1994).

A three-dimensional (3D) analysis is beyond the scope of the present paper, but may probably be carried out using a good dataset with seismics and multiple deviated wells, using parameters as e.g. ‘throw’ variations along traces of deviated wells. The density of 3D deviated well coverage may, however, be at a larger scale than that of relative homogenous or simple populations of microfaults.

Such an analysis is of economic interest because it may give better estimates of hydrocarbon reserves in discoveries with limited seismic resolution and a limited number of wells.

The normal fault data are used in the thickness calculations to describe bulk properties of the region of investigation (cf. Jamison and Stearns, 1982). The formulas below are derived by assuming that the faults are regularly spaced and all with the same displacement, as in the domino model of Wernicke and Burchfiel (1982), and analysed in terms of pure and simple shear, with the possibility of interpolation.

\* Corresponding author.

E-mail address: spal@statoil.com (S. Pallesen).

### Nomenclature

|                  |   |
|------------------|---|
| $d_m$            | mean dip-slip displacement on faults  |
| $N$              | recalculated number of faults in orthogonal section                           |
| $N_{\text{obs}}$ | number of faults observed in deviated well                                    |
| $S_h$            | mean fault spacing along deformed surface                                     |
| $S_v$            | vertical fault spacing  |
| $t_0$            | original layer thickness  |
| $t_{\text{obs}}$ | thickness of stretched/sheared layer  |
| $T$              | throw, relative to the original bedding surface, for a single 'typical' fault |
| $x$              | initial length of part of fault plane cutting the layer                       |
| $\alpha$         | dip of a layer  |
| $\beta$          | equal-area (plane strain) stretching and thinning factor                      |
| $\delta$         | plunge of well trace  |
| $\Delta T$       | total thinning; sums of throws in orthogonal section                          |
| $\Delta t_m$     | mean throw for faults in orthogonal section                                   |
| $\phi_i$         | fault dip   |
| $\psi$           | shear angle   |

The application of formulas derived from an ideal population (Figs. 1–5) using core data with variations in fault densities and displacements is discussed under pure and simple shear models, respectively.

The simplified modelling suggested here probably applies best to local layers (reservoirs) of massive sandstone at the scale of the case study (a few tens of metres of thickness) because, for the case of interbedded sand–shale reservoir formations, there is the possibility that subtle changes in mechanical properties may cause a more complex micro-fault pattern. This would make a uniform model less justifi-

able. Very long cores may incorporate several distinct strain zones and different structural styles. Size limitations on deformation bands due to strain hardening (cf. Fossen and Hesthammer, 1997) may, on the other hand, contribute to a partially homogeneous distribution of microfaults.

## 2. Registration of data

The methods of structural core logging have been described in general in several publications (e.g. Gabrielsen and Koestler, 1987; Kulander et al., 1990), and will not be dealt with here.

We first write down: (i) numbers of faults per unit length of core, (ii) displacements on individual faults, and (iii)

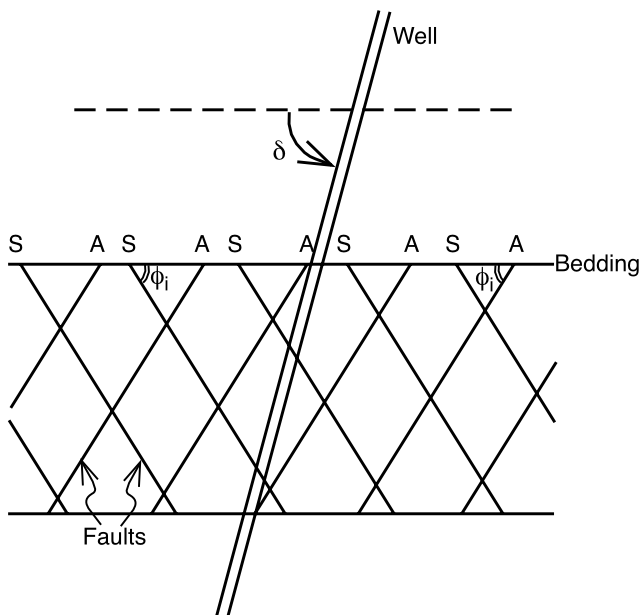


Fig. 1. Illustration to show how number of faults encountered vary with the plunge of the well trace ( $\delta$ ) and the fault angle ( $\phi_i$ ) in application of a pure-shear model.

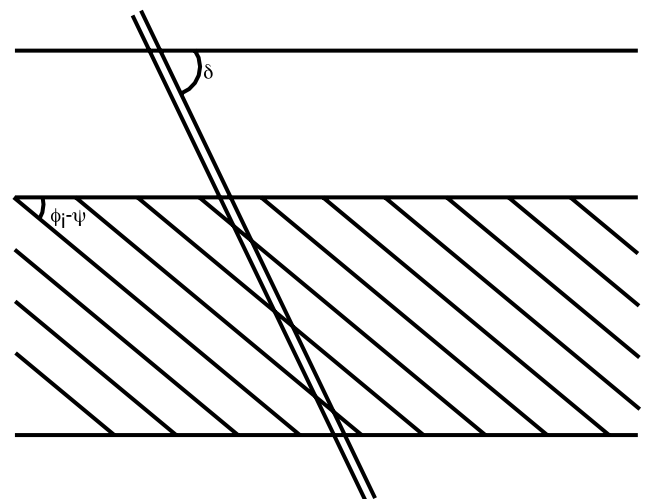


Fig. 2. Illustration to show how number of encountered faults vary with the plunge of the well trace ( $\delta$ ), the initial fault angle ( $\phi_i$ ), and the shear angle ( $\psi$ ) in application of a simple-shear model.

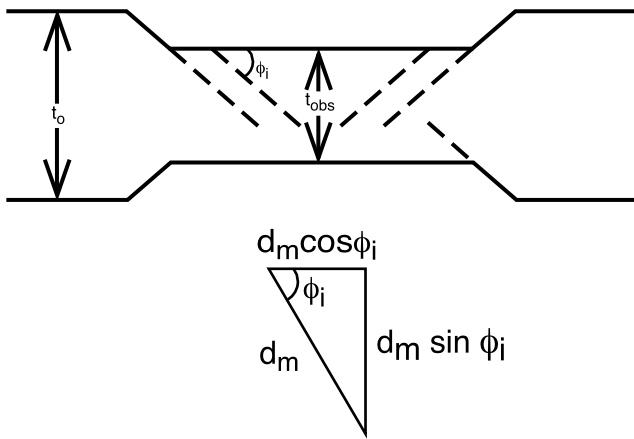


Fig. 3. Sketch to show how a section is thinned by pure shear. The fault angle is  $\phi_i$ , and the mean displacement is  $d_m$ .

whether the faults dip in one or two directions (or draw sketches of faults in each core length). Induced fractures are not included—see Kulander et al. (1990) on how induced fractures differ from natural ones.

Then the total number of faults is summed, compensating for the missing core. In the case study, compensation for the missing core due to sampling was carried out locally for each metre of core. The cores were located in boxes as 1-m lengths. If 20 cm of 1 m of core was missing, then the number of microfaults encountered for the remaining 80 cm of core was divided by 0.8 to obtain the compensated number of microfaults for the whole metre of core.

Furthermore, the mean observed displacement was calculated. In the description given here, including the case study, the displacement is measured directly from the slabbed core surface. This may, however, sometimes give erroneous data because the core is not always slabbed in the original vertical position. An alternative method which may be applied to deviated wells in general, is to use ‘throw’ along the core axis. This may be recalculated to find vertical throw or ‘throw’ in any direction.

The well deviation angle is noted from the well report. The well plunge used below is complementary to the well

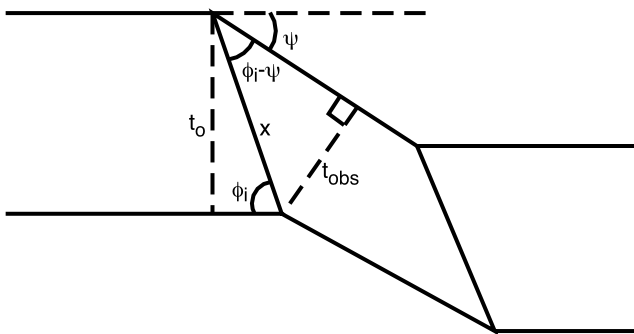


Fig. 4. This figure shows some of the parameters used in the simple-shear model. See text for explanation.

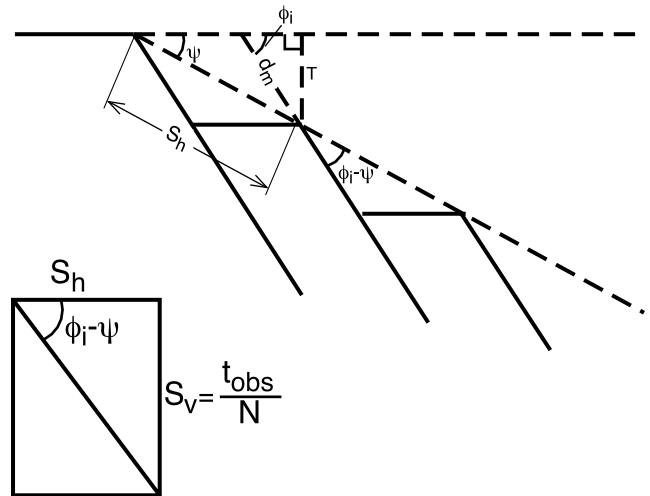


Fig. 5. A further set of parameters used in the simple-shear model. See text for explanation.

deviation. If the layer is not flat-lying, then the well plunge is used relative to the bedding.

### 3. Calculation of layer–orthogonal fault intensity from well deviation

#### 3.1. Introductory remark

The orthogonal microfault intensity is needed in the calculations because we wish to calculate the undeformed orthogonal thickness (isopach) of the layer we study. A 3D structural setting may often be treated in a 2D model, as described here. Furthermore, the recalculations and parameter used here basically reduces the 2D modelling to one-dimensional (1D) calculations in terms of correcting the orthogonal thickness. Thus a deviated hole can be corrected to determine the thinning. The data are treated in terms of end-member models (pure and simple shear), with possibilities of interpolation.

#### 3.2. Pure-shear case

In this case, the faults are assumed to be distributed uniformly, with equal amounts of synthetic and antithetic (conjugate) faults. The number of faults observed in the core is termed  $N_{obs}$ . We assume that faults are dipping  $\phi_i$  degrees (in opposite directions). Then the recalculated number of faults encountered in an orthogonal well ( $N$ ) relative to plunge of well ( $\delta$ ) (in the range  $0–180^\circ$ ) is (Fig. 1):

$$\begin{aligned}
 N &= N_{obs} [|\sin(90^\circ - \phi_i)| + |\sin(90^\circ - (180^\circ - \phi_i))|] / [|\sin(\delta - \phi_i)| + |\sin(\delta - (180^\circ - \phi_i))|] \\
 &= N_{obs} [2\cos\phi_i] / [|\sin(\delta - \phi_i)| + |\sin(\delta + \phi_i)|] \quad (1)
 \end{aligned}$$

(The orthogonal well is related to orthogonal thickness (isopach), which again is important in hydrocarbon volume calculations or as input to seismic interpretation.)

### 3.3. Simple-shear case

In the case of simple-shear, all faults are set to dip in one direction. The number of faults encountered in an orthogonal well ( $N$ ) is now a function of both well deviation ( $\delta$ ), fault initial dip ( $\phi_i$ ) and shear angle ( $\psi$ ) (Fig. 2);

$$N = N_{\text{obs}} \sin(90^\circ - (\phi_i - \psi)) / \sin(\delta - (\phi_i - \psi))$$

$$= N_{\text{obs}} \cos(\phi_i - \psi) / \sin(\delta - (\phi_i - \psi)) \quad (2)$$

Using this method, the relative orientation of fault dip and the well is selected.

### 4. Local pure-shear model

The well section consists of  $N$  normal faults, with mean dip-slip displacement  $d_m$  and mean throw  $\Delta t_m$  (Fig. 3):

$$\Delta t_m = d_m \sin \phi_i \quad (3)$$

Now throw equals missing vertical section, which is equal to absolute thinning. For the entire orthogonal thickness, the total thinning  $\Delta T$  is:

$$\Delta T = N d_m \sin \phi_i \quad (4)$$

McKenzie (1978) defined a stretching/thinning factor  $\beta$  in which  $\beta = 1$  corresponds to no thinning, and  $\beta = 2$  implies a new thickness as the half of the old thickness. In our case, we have:

$$\beta = (t_{\text{obs}} + N d_m \sin \phi_i) / t_{\text{obs}} \quad (5)$$

and the original thickness is:

$$t_0 = t_{\text{obs}} + N d_m \sin \phi_i \quad (6)$$

The use of the formulas above derived from an ideal pure-shear model on real data showing that variations in spacing and displacement are unproblematic, because the thinning calculation in Eq. (6) below—using mean throw—can be replaced by successive additions of throws for each micro-fault (with varying size), which gives the same result.

### 5. Local simple-shear model

In a local simple shear model, a large number of faults dip in the same direction, and are equally spaced and displaced (Fig. 4).

For the case of pure shear on a larger scale, we may have local zones of simple shear (e.g. drag effects near large faults or in rollovers), as in a continental rift. The terms ‘pure shear’ and ‘simple shear’, however, in the present context refer to the region under investigation.

The zone of faulting is limited by two ‘boundary’ faults. The original thickness is  $t_0$ , and the orthogonal thickness of the deformed zone is  $t_{\text{obs}}$ . Note that the deformed layer dips relative to the undisturbed layer (as in e.g. a drag zone). During deformation, the disturbed layer has been stretched parallel to the disturbed bedding by a factor  $\beta$ . Using the principle of area conservation, we get, as above:

$$t_0 = \beta t_{\text{obs}} \quad (7)$$

The original parallelogram with  $\phi_i$  and  $180^\circ - \phi_i$  degree angles has been deformed into more acute and obtuse angles  $\phi_i - \psi$  and  $180^\circ - \phi_i + \psi$ , where  $\psi$  is the shear angle

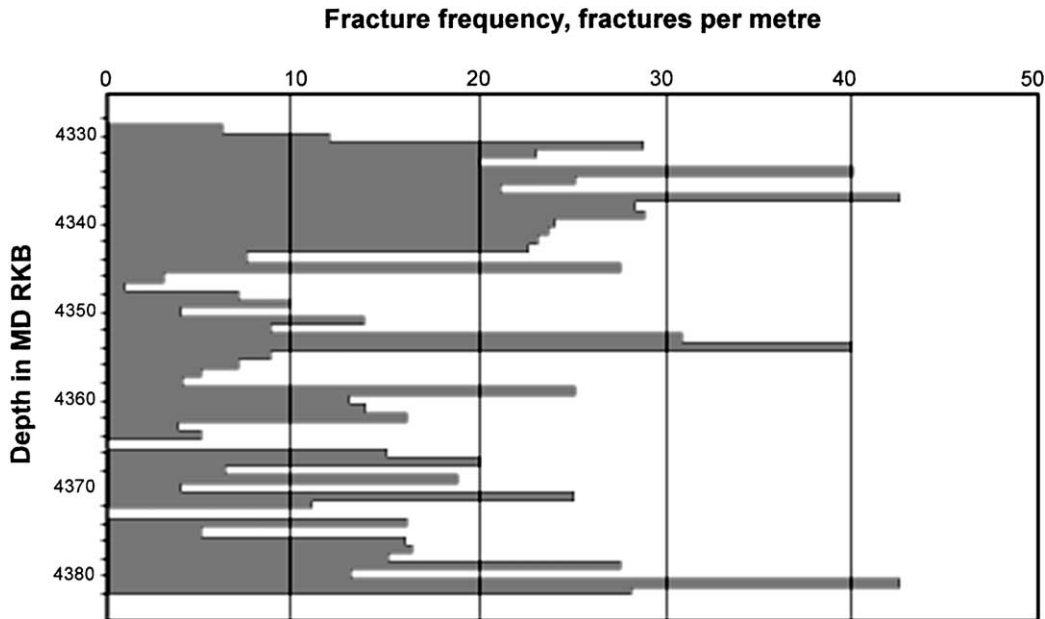


Fig. 6. Number of microfaults per metre of core for a North Sea well. The figures have been corrected for missing core (see text).

Table 1  
Data and results for case study

|   |       |
|---|-------|
| Data  |       |
| Length of core (excluding 3 m with synsed. deformation); m              | 52    |
| Orthogonal thickness of cored section ( $t_{\text{obs}}$ ); m           | 40    |
| Plunge of well trace ( $\delta$ ); degrees                              | 50    |
| Observed number of faults ( $N_{\text{obs}}$ )                          | 829   |
| Estimated fault dip ( $\phi_i$ ); degrees                               | 60    |
| Mean displacement (based on 42 measurements); m                         | 0.031 |
| Pure-shear model  |       |
| Recalculated number of faults ( $N$ )                                   | 744   |
| Stretching/thinning factor ( $\beta$ )                                  | 1.50  |
| Undeformed orthogonal thickness of core ( $t_0$ ); m                    | 59.8  |
| Simple-shear model  |       |
| Recalculated number of faults ( $N$ )                                   | 642   |
| Shear angle ( $\psi$ ); degrees   | 20.7  |
| Stretching/thinning factor ( $\beta$ )                                  | 1.37  |
| Undeformed orthogonal thickness of core ( $t_0$ ); m                    | 54.5  |
| Application to the Hugin Formation                                      |       |
| Reservoir present-day orthogonal thickness; m                           | 18.0  |
| Undeformed thickness (pure-shear model); m                              | 27.0  |
| Undeformed thickness (simple-shear model); m                            | 24.7  |
| Ratio of synthetic (roughly parallel to core axis) to antithetic faults |       |
| (roughly normal to core axis)   | 0.5   |
| Interpolated ('mixed') model of undeformed thickness; m                 | 25.5  |

(Fig. 4). The faults do not dip  $\phi_i$  degrees relative to the disturbed bedding, they dip  $\phi_i - \psi$  degrees.

The initial length of the part of the fault plane cutting the reservoir ( $x$ ), is

$$x = t_0 / \sin(\phi_i) \quad (8)$$

At the same time,  $x$  can be calculated from deformed thickness and shear angle  $\psi$  (Fig. 4):

$$x = t_{\text{obs}} / \sin(\phi_i - \psi) \quad (9)$$

Combining Eqs. (8) and (9), and letting  $\beta = t_0 / t_{\text{obs}}$ , we get:

$$\beta = \sin \phi_i / \sin(\phi_i - \psi) \quad (10)$$

or

$$t_0 = t_{\text{obs}} \sin \phi_i / \sin(\phi_i - \psi) \quad (11)$$

In Eq. (11), there are two unknowns, viz.  $t_0$  and  $\psi$ . To find  $\psi$ , we apply the known parameters  $d_m$  (mean displacement) and  $N$  (numbers of faults), which are not included in Eq. (11).

This Eq. (11) is in principle the same equation as used by Wernicke and Burchfiel (1982) for estimating extension from a series of rotated fault blocks. See Fig. 5. We now define:

$$T = d_m \sin \phi_i \quad (12)$$

where  $T$  is the the throw, relative to original bedding

surface, for a single fault. Furthermore:

$$S_h = t_{\text{obs}} / (N \tan(\phi_i - \psi)) \quad (13)$$

where  $S_h$  is the fault spacing along the disturbed surface. Because we see from Fig. 5 that:

$$\sin \psi = T / S_h \quad (14)$$

we find the shear angle ( $\psi$ ) expressed implicit by a non-linear equation:

$$\sin \psi / \tan(\phi_i - \psi) = d_m \sin \phi_i N / t_{\text{obs}} \quad (15)$$

which can be solved numerically by minimizing  $|f(\psi)|$ , where  $f(\psi)$  is the left side minus the right side of Eq. (15).

Yet another iteration may be used: we had to input  $\psi$  in the start in Eq. (2) to get an expression for number of faults in an orthogonal section ( $N$ ). Starting with Eq. (2) and  $\psi = 0$ , we proceed to Eq. (15) to find a new value of  $\psi$  and then, going back to Eq. (2) we proceed to Eq. (15) again, for a suitable number of iterations. After we have found  $\psi$ , we input its value into Eq. (11) and find the original layer thickness.

The use of the equations above from the ideal model on real data showing variations in spacing and displacements seems to work in practice. The thinning of the layer in simple shear is the result of a sum of throw increments (each valued  $d_m \sin(\phi_i - \psi)$ ) in which  $\psi$  increases for each increment of  $d_m$ . It is probable that  $\psi$  may be regarded as a bulk property (a function of total throw) of the region of study as long as the microfaults are small relative to the layer thickness.

A couple of computer tests were run to see if there were changes in the result for the thinning estimate if a cored section data was subdivided in two. This was carried out to see if the results from the subsets added together gave the same result as for the cored section as a whole, as a check on the effect of heterogeneity.

The starting point was a section with  $N = 1000$  micro-faults, a mean displacement of  $d_m = 0.05$  m, and an original thickness of  $t_{\text{obs}} = 50$  m. This gave, using  $\phi_i = 60^\circ$  and  $\delta = 90^\circ$ , an original thickness of  $t_0 = 86$  m. A first subdivision with ( $N = 400$ ,  $d_m = 0.06$  m,  $t_{\text{obs}} = 25$  m) combined with ( $N = 600$ ,  $d_m = 0.0433$  m,  $t_{\text{obs}} = 25$  m) (the same combined weighted mean displacement of 0.05 m as for the 1000 m interval) gave, in combination, an original thickness of  $t_0 = 86$  m, the same as above. A second subdivision ( $N = 100$ ,  $d_m = 0.07$  m,  $t_{\text{obs}} = 25$  m) combined with ( $N = 900$ ,  $d_m = 0.0478$ ,  $t_{\text{obs}} = 25$  m) (combined weighted mean of  $d_m = 0.05$  m) gave original thickness  $t_0 = 87$  m. Thus the method seems to be robust to variations within a dataset for given overall (bulk) properties.

## 6. Case study

The case study well was the first exploration well drilled on a prospect in the Norwegian North Sea, with the Upper

Jurassic Hugin Formation as a target. Oil was found. The drilled reservoir thickness was, however, disappointingly low. Inspection of the core revealed a high number of microfaults (deformation bands, granulation seams). These were used to calculate a representative reservoir thickness for the prospect.

Structural core logging was carried out on two cores, covering the lower part of the Hugin Formation, and the uppermost part of the Triassic Skagerrak Formation. The natural fractures were observed to be microfaults. These had displacements from a few millimetres to a few centimetres, many of them with grain-size reduction as seen in the microscope. Microfault frequencies in the cores were found to be very high, and are given in Fig. 6.

All microfaults were assumed to strike parallel to the main fault in the area (in a synthetic or antithetic sense), thus reducing the work to a 2D analysis. The models given above for pure and simple shear were regarded as end-member models for a situation in which microfault orientation was unknown in detail.

Data and results from the modelling are given in Table 1. Given the observed faulted Hugin Formation vertical thickness of 18.0 m, the application of the above model gives: (i) an unfaulted thickness of 27.0 m (150%) when a pure-shear model is applied, (ii) an unfaulted thickness of 24.7 m (137%) for simple shear, and (iii) an unfaulted thickness of 25.5 m (142%) for a mixed model. The interpolation between pure and simple shear was based upon drawings of core microfaults at a scale of 1:5, showing a partial asymmetric orientation of microfaults (as synthetic or antithetic, respectively).

The results were found to be highly sensitive to the mean displacement on microfaults. In the case study, the mean displacement was found from a limited number of observations (42), which is small relative to the observed number of microfaults (829). The limited number of observations was caused by partial absence of strain markers due to the often massive character of the Hugin Formation sandstone.

## 7. Discussion and conclusions

Tectonic thinning of layers can be calculated using the methods above. High intensities of microfaults or deformation bands (which can be studied using core data or outcrops) are usually but not always found in the vicinity of major faults (Antonellini et al., 1994). Thus a thinning estimate based on microfaults is a minimum estimate because of core dimensions and the fact that dipmeter data are not always available.

This paper addresses bulk strain of a studied column. Within that column, however, the relative thinning (e.g. per metre) may vary with microfault densities and throws, which would also effect variations in extensional structures and structural style.

The limitations of this method are: (i) the assumption that

the actual strain can be modelled in 2D, (ii) data collection problems from the core (larger faults, possible absence of strain markers in massive rock, displacement measurements, some ‘faults’ may be joints or induced fractures), and (iii) the use of a strain model for an interval, which may be structurally complex or may have had multiphase deformation.

Westaway and Kusznir (1993) argued that rotation of faults and bedding in fault blocks is caused by simple shear rather than rigid-body rotation. If this is the case, a considerable of ‘background’ faulting should be present in rotated blocks.

A future challenge would be to use the simple-shear model with well data integrated with Mandl’s (1988, p. 52) model of antithetic fault spacing. In the present model of simple shear, fault spacing is linked to thinning and number of microfaults. In Mandl’s (1988) model, antithetic fault spacing is linked to depth to master fault.

Another challenge would be to calculate optimum deviation angle ( $\delta$ ) for another well close to one previously studied, which intersects a maximum of faults if this may increase fluid flow (well productivity).

Finally, it should be mentioned that the formulas given above are for a flat-laying layer (Figs. 1 and 2), in which the vertical thickness (isochor) equals the orthogonal thickness (isopach). However, if the layer is dipping by an angle  $\alpha$ , then the formulas above are valid for the isochor only, and a last-step correction to find the isopach is carried out by multiplying the isochor by the cosine of  $\alpha$ .

## Acknowledgements

R.H. Gabrielsen and J. Korstgård commented on an early draft. The referees (J.P. Evans and B. Kulander) are thanked for comments that helped improve the manuscript. Statoil is thanked for support and permission to publish.

## References

- Antonellini, M.A., Aydin, A., Pollard, D., 1994. Microstructure of deformation bands in porous sandstones at Arches National Park, Utah. *Journal of Structural Geology* 16, 941–959.
- Fossen, H., Hesthammer, J., 1997. Geometric analysis and scaling relations of deformation bands in porous sandstone. *Journal of Structural Geology* 19, 1479–1493.
- Gabrielsen, R.H., Koestler, A.G., 1987. Description and structural implications of fractures in late Jurassic sandstones of the Troll Field, northern North Sea. *Norsk Geologisk Tidsskrift* 67, 37–381.
- Hesthammer, J., 1998. Integrated use of well data for structural control of seismic interpretation. *Petroleum and Geoscience* 4, 97–109.
- Jamison, W.R., Stearns, D.W., 1982. Tectonic deformation of the Wingate Sandstone, Colorado National Monument. *AAPG Bulletin* 66, 2584–2608.
- Kulander, B.R., Dean, S.L., Ward Jr, B.J., 1990. Fractured Core Analysis: Interpretation, Logging, and Use of Natural and Induced Fractures in Core. *AAPG Methods in Exploration Series*, No. 8. American Association of Petroleum Geologists, Tulsa, Oklahoma.

- Mandl, G., 1988. *Mechanics of Tectonic Faulting. Models and Basic Concepts*. Elsevier, Amsterdam.
- McKenzie, D., 1978. Some remarks on the evolution of sedimentary basins. *Earth and Planetary Science Letters* 40, 1197–1211.
- Underhill, J.R., Woodcock, N.H., 1987. Faulting mechanisms in high-porosity sandstones; New Red Sandstone, Arran, Scotland. In: Jones, M.E., Preston, R.M.F. (Eds.), *Deformation of Sediments and Sedimentary Rocks*. Geological Society, London, Special Publication 29, pp. 91–105.
- Wernicke, B., Burchfiel, B.C., 1982. Modes of extensional tectonics. *Journal of Structural Geology* 4, 105–115.
- Westaway, R., Kusznir, N., 1993. Fault and bed ‘rotation’ during continental extension: block rotation or vertical shear? *Journal of Structural Geology* 15, 753–770.